Galaxies at $z \sim 7 - 8$: z_{850}-dropouts in the Hubble Ultra Deep Field

R.J. Bouwens[2], R.I. Thompson[3], G.D. Illingworth[2], M. Franx[4], P. van Dokkum[5], X. Fan[3], M.E. Dickinson[6], D.J. Eisenstein[3], M.J. Rieke[3]

1 Based on observations made with the NASA/ESA Hubble Space Telescope, which is operated by the Association of Universities for Research in Astronomy, Inc., under NASA contract NAS 5-26555.

2 Astronomy Department,University of California, Santa Cruz, CA 95064

3 Steward Observatory, University of Arizona, Tucson, AZ 85721.

4 Leiden Observatory, Postbus 9513, 2300 RA Leiden, Netherlands.

5 Department of Astronomy, Yale University, New Haven, CT 06520.

6 National Optical Astronomy Obs., P.O. Box 26732, Tucson, AZ 85726.

ABSTRACT

We have detected likely $z \sim 7 - 8$ galaxies in the $144'' \times 144''$ NICMOS observations of the Hubble Ultra Deep Field. Objects are required to be $\geq 3\sigma$ detections in both NICMOS bands, J_{110} and H_{160}. The selection criteria for this sample are $(z_{850} - J_{110})_{AB} > 0.8$, $(z_{850} - J_{110})_{AB} > 0.66(J_{110} - H_{160})_{AB} + 0.8$, $(J_{110} - H_{160})_{AB} < 1.2$, and no detection at $< 8500\mathring{A}$. The 5 selected sources have total magnitudes $H_{160,AB} \sim 27$. Four of the five sources are quite blue compared to typical lower–redshift dropout galaxies and are clustered within a $1\,\square'$ region. Because all 5 sources are near the limit of the NICMOS data, we have carefully evaluated their reality. Each of the candidates is visible in different splits of the data and a median stack. We analyzed several noise images and estimate the number of spurious sources to be 1 ± 1. A search using an independent reduction of this same data set clearly revealed 3 of the 5 candidates and weakly detected a 4th candidate, suggesting the contamination could be higher. For comparison with predictions from lower redshift samples we take a conservative approach and adopt four $z \sim 7 - 8$ galaxies as our sample. With the same detection criteria on simulated datasets, assuming no-evolution from $z \sim 3.8$, we predict 10 sources at $z \sim 7 - 8$, or 14 if we use a more realistic $(1 + z)^{-1}$ size scaling. We estimate that the rest-frame continuum UV ($\sim 1800\mathring{A}$) luminosity density at $z \sim 7.5$ (integrated down to $0.3L^*_{z=3}$) is just $0.20^{+0.12}_{-0.08}\times$ that found at

$z \sim 3.8$ (or $0.20^{+0.23}_{-0.12} \times$ including cosmic variance). Effectively this sets an upper limit on the luminosity density down to $0.3 L^*_{z=3}$. This result is consistent with significant evolution at the bright end of the luminosity function from $z \sim 7.5$ to $z \sim 3.8$. Even with the lower UV luminosity density at $z \sim 7.5$, it appears that galaxies could still play an important role in reionization at these redshifts, though definitive measurements remain to be made.

Subject headings: galaxies: evolution — galaxies: high-redshift

1. Introduction

From the spectroscopic identification of a population of $z \sim 3$ dropouts (Steidel et al. 1996) to recent work on i-dropouts (Yan et al. 2003; Stanway et al. 2003; Bouwens et al. 2003b; Dickinson et al. 2004), the frontier for high redshift galaxy studies is continually being redefined. In this paper, we extend this frontier to $z \sim 7$ and beyond by performing a z_{850}-dropout search over the area of the Hubble Ultra Deep Field (Beckwith et al. 2004) with deep NICMOS coverage (Thompson et al. 2004a). The exceptional depth of both the optical and infrared data makes this area ideal for carrying out such a search, reaching to 29.5, 29.7, 29.4, 28.8, 27.6, and 27.4 (5σ, $0.6''$-diameter apertures) in the $F435W$, $F606W$, $F775W$, $F850LP$, $F110W$, and $F160W$ bands (hereinafter, B_{435}, V_{606}, i_{775}, z_{850}, J_{110} and H_{160}, respectively.) Previously, this redshift range had been probed by an I_{814}-dropout search in the HDF-North (Dickinson 2000) and similar dropout searches around lensing clusters (Kneib et al. 2004; Pelló et al. 2004). All magnitudes are expressed in the AB system. We assume $(\Omega_M, \Omega_\Lambda, h) = (0.3, 0.7, 0.7)$ (Bennett et al. 2003).

2. Analysis

Our search area was the $0.09''$ pixel $144'' \times 144''$ NICMOS mosaic (Thompson et al. 2004a). Sources were identified in the summed $J + H$ image (RT) and the χ^2 (Szalay et al. 1999) image (RB) using the SExtractor code (Bertin & Arnouts 1996). Colors were calculated using a scaled aperture Kron magnitude (1980) with the Kron factor equal to 1.2. Total magnitudes were then derived using the χ^2 image to correct these fluxes to a much larger aperture (where the Kron factor was equal to 2.5) (see Bouwens et al. 2003a). Typical corrections were ~ 0.8 mag for each object.

(a) z_{850}-dropout selection. Objects were required to be null detections ($< 2\sigma$) in the deepest (V_{606} and i_{775}) optical bands (in $0.6''$-diameter apertures), and lie in the expected

place $[(z_{850} - J_{110}) > 0.8, (z_{850} - J_{110})_{AB} > 0.66(J_{110} - H_{160})_{AB} + 0.8, (J_{110} - H_{160})_{AB} < 1.2]$ in the standard two-colour $z_{850} - J_{110}/J_{110} - H_{160}$ diagram. To clean our catalog of possible spurious detections, objects were required to be 3σ detections ($0.6''$-diameter aperture) in both the J_{110} and H_{160} bands. These procedures identified a set of 8 sources to a limiting magnitude of $H_{160,AB} \sim 28$. A separate selection by RT identified a similar set of objects. After identification, each source was located in the original exposures (16 in each band) to ensure that they did not arise from a small subset of the exposures (e.g., from a pre-integration cosmic ray hit). Three of our 8 sources were rejected, being visible in only a couple of exposures. The 5 real sources are shown in Figure 1 and Table 1.

Table 1 includes the photometric information for our 5 candidates plus one red galaxy which nearly met our criteria (this latter object was also found by Yan & Windhorst 2004). Candidates had $H_{160,AB}$ magnitudes ranging from 26.0 to 27.3, or 0.5-1.5 times the characteristic rest-frame UV luminosity (L^*) for Lyman break galaxies at $z \sim 3$ (Steidel et al. 1999). Candidates appear to be rather clustered, with 4 of the 5 candidates falling within a $\sim 1\,\square'$ area. Figure 2 displays postage stamp images of each candidate along with its position in color-color space and an SED fit to the broadband fluxes.

(b) *Testing Source Reality.* Our 5 candidates were then subjected to several additional tests. Each source was verified to exist at the $> 2.5\sigma$ level in the $J + H$ image for each of the two epochs (taken two months apart and at a 90 degree angle to each other). Each source was also evident ($> 2.4\sigma$) in a median stacking of the 16 overlapping exposures for each band. This is useful since the median process should eliminate sources with flux in only a few exposures. After performing the above sanity checks on our candidates, we repeated our selection procedure on three different images sets to examine the likelihood that our candidates are simply spurious detections. These three images include the "negative" images, the first epoch images subtracted from the second epoch images, and the second epoch images subtracted from the first. These images should have similar noise characteristics to the data, but contain no real sources. Only 1, 2, and 0 objects, respectively, were found on each of the above three image sets (5.76 arcmin^2) using an identical selection procedure. This suggested a small level of contamination from spurious sources (1 ± 1 object) in the current sample.

(c) *An Independent Check on Source Reality.* An independent reduction of the NICMOS images was kindly made available to one of us (RT) by Robberto et al. (2004). The image was inspected by RT and 3 of our 5 candidate sources clearly appear in those images. However, no signal is evident at the position of UDF-818-886, while UDF-491-880 is only weakly detected. Until this is resolved, the contamination may be higher than estimated above (§2b).

(d) *Low-Redshift Contamination.* To test for possible contamination from low-redshift interlopers, we randomly assigned the colors of bright ($23.5 < H_{160,AB} < 25$) objects from

the UDF to faint objects in our field, added photometric scatter, and then repeated our selection. No objects were found, suggesting minimal contamination from low-redshift interlopers. Possible contamination from T dwarfs was also considered, given their position in color-color space (Figure 1) and predicted numbers (0.04-0.3 objects) over our field of view (Burgasser et al. 2004). However, this proved not to be a concern for our sample, since T dwarfs would appear as $\gtrsim 5\sigma$ point sources in the deep z_{850}-band images, and none were found.

(e) Expected Numbers/Incompleteness Tests. It is interesting to compare the number of candidates against that predicted assuming no-evolution from lower redshift. As in other recent work, we adopt a $z \sim 3.8$ *B*-dropout sample from the GOODS fields (Bouwens et al. 2004, hereinafter B04) as our reference point and project it to $z \sim 6 - 10$ using our well-established cloning machinery (Bouwens et al. 1998a,b; Bouwens et al. 2003a; B04). Such simulations are important for establishing the incompleteness, which can be as high as 75% for these $z \sim 7-8$ objects (this includes the effect of possible blending with foreground galaxies). Adding the cloned galaxies directly to the data, we repeat our selection procedure and thereby derive a no-evolution prediction; this yields 10 dropouts. However, we know that galaxies evolve in size (a $(1 + z)^{-1}$ size scaling for fixed luminosity: Bouwens et al. 2004a,c; Ferguson et al. 2004) and hence surface brightness. Including this effect, 14 objects are found. Steeper size scalings (e.g., $(1 + z)^{-2}$) yield still larger values (~ 18 objects) while using bluer colors (e.g., UV slopes $\beta \sim -2.5$) has little effect on the predictions.

(f) Source Characteristics / Possible Concerns. Given the depth of the UDF z_{850}-band imaging, it was somewhat surprising that only 1 of our 5 candidates is detected in this band. We used the simulations described above (§2e) to quantify this and found that 58%, or 2.9 of our 5 candidates, should be detected at $> 2\sigma$ in the z_{850}-band. A single detection in z_{850} has only a 10-22% likelihood of occurrence, the larger number for significant clustering. Four of the objects are spatially clustered, falling within a $1\,\square'$ area. Such clustering is not unexpected, and the lack of z_{850}-band flux would result if they are also at $z > 7.5$.

These 4 clustered objects are also quite blue, relative to the fiducial 10^8 yr starburst, though the significance of this result is modest ($< 2\sigma$). Their rest-frame UV colors (with $\beta \sim -3$) are bluer than typical dropouts at both $z \sim 3$ (Steidel et al. 1999) and $z \sim 6$ (Stanway et al. 2004b) where $\beta \gtrsim -2.2$ (the $E(B - V) \gtrsim 0$ track in Figure 1). If real, they are also bluer than one would expect from models which give $\beta \gtrsim -2.5$ regardless of age, dust, or metallicity content, including population III objects (Schaerer 2003; Venkatesan et al. 2003). However, such blue colors are not completely unknown at $z \sim 3$ (e.g., Adelberger & Steidel 2000). They also might arise from a significant contribution of Ly-α emission (rest-frame EWs $\gtrsim 200\text{\AA}$) to the J_{110}-band flux.

The one red object in our $z \sim 7 - 8$ sample has colors that are also consistent with a $z \sim 1$ galaxy, though it would be rather unusual, needing to be a compact ($\sim$ 1kpc), significantly reddened, old stellar population dwarf galaxy, > 6 magnitudes fainter that L^*; we consider it more likely to be at high redshift.

3. Luminosity Density and Implications

We are now prepared to compare the observations with the predictions made earlier (§2e). This will permit us to set important constraints on the evolution at the bright end of the luminosity function in rest-frame continuum-UV ($\sim 1800\text{Å}$) and therefore make inferences about changes in the luminosity density. To be conservative, we shall assume the number of z_{850}-dropouts is four. Given possible concerns about their validity (§2b;§2c;§2f), we will also consider the implications if there are even fewer sources. For the expected number of z_{850}-dropouts, we use 14, the prediction from the $(1 + z)^{-1}$ size scaling (§2e).

Comparing our 4 fiducial candidates with the 14 objects predicted suggests that the number of objects at the bright end of the LF at $z \sim 7.5$ is just $0.29\times$ that at $z \sim 3.8$ (Figure 3). This decreases to $0.14\times$ and $< 0.13\times$ (1σ) if only two or none of our candidates are real, respectively. Obviously, there are substantial uncertainties in the estimated shortfall, both as a result of the small number statistics and the expected cosmic variance (factor of 2: assuming a CDM power spectrum normalized to high redshift observations and a redshift selection window of unit width, e.g., Somerville et al. 2004). Therefore, even no evolution is consistent with the present result at the 1.5σ level.

While a number of options are open, the most likely case is a drop of at least $3.5\times$ in the number of objects at the bright end of the LF. Since this is similar to what is found at $z \sim 6$ (Stanway et al. 2003; Dickinson et al. 2004; Stanway et al. 2004a), it is likely a continuation of the same effect. A key question is whether the observed deficit continues all the way down the luminosity function or if it is due to evolution in the characteristic luminosity (L^*) at high redshift. This whole issue is pivotal for questions about reionization since it is at faint magnitudes that the bulk of the flux arises (assuming a steep $\lesssim -1.5$ faint-end slope α). Fortunately, the fainter i-dropouts from the UDF are beginning to provide us with some clues, and some early studies are already suggesting that the principal form of the evolution is in luminosity or a steepening of the faint-end slope (Dickinson et al. 2004; Yan & Windhorst 2004; Bouwens et al. 2004d; cf. Bunker et al. 2004). If true, this would provide a natural explanation for our shortfall and may allow for substantial star formation at higher redshifts as suggested by recent measurements from WMAP (Kogut et al. 2003) or the large stellar masses found in the $z \sim 6.5$ Kneib et al. (2004) object (Egami et al. 2004).

It would also suggest that for a proper census of these objects the present surveys need to be extended to considerably fainter magnitudes (with WFC3 and ultimately with JWST).

In light of the uncertainties regarding the form of the evolution, we have chosen simply to quote the evolution in luminosity density down to the total magnitude limit of our survey ($H_{160,AB} \sim 27.5$, or $\sim 0.3L^*_{z=3}$). Conversions to star formation rate density (uncorrected for extinction) are made using the now canonical conversion factors for the Salpeter IMF (Madau et al. 1998). For both quantities (the luminosity density and the star formation rate), we infer a larger drop than above (due to luminosity-weighting). To the faint end limit and including the Poissonian variations quoted above, we find that $\rho(UV, z = 7.5)/\rho(UV, z = 3.8) = 0.20^{+0.12}_{-0.08}$ using our fiducial list of candidates and $0.10^{+0.09}_{-0.05}$ and < 0.05 (1σ) assuming only two or none of our candidates are real, respectively. Uncertainties on these quoted factors increase to $0.20^{+0.23}_{-0.12}$, $0.10^{+0.20}_{-0.07}$, and < 0.11 (1σ), respectively, including the expected field-to-field variations (cosmic variance) quoted above. Figure 3 shows a comparison of these results with those at lower redshift.

This is the first such deep sample ever compiled at $z \sim 7 - 8$ and allowed us to set some constraints on the bright end of the rest-frame UV-continuum luminosity function at $z \sim 7.5$, during the epoch of reionization. The similarity of the present result with that at $z \sim 6$ (Stiavelli et al. 2004; Yan & Windhorst 2004) suggests that galaxies could have been an important contributor to reionization at these early times, though a characterization of their role warrants more definitive measurements.

REFERENCES

Adelberger, K. L. & Steidel, C. C. 2000, ApJ, 544, 218.

Beckwith, S. V. W. et al. 2004, in preparation.

Bennett, C. L. et al. 2003, ApJ, 583, 1.

Bertin, E. and Arnouts, S. 1996, A&AS, 117, 393.

Bouwens, R., Broadhurst, T. and Silk, J. 1998a, ApJ, 506, 557.

Bouwens, R., Broadhurst, T. and Silk, J. 1998b, ApJ, 506, 579.

Bouwens, R., Broadhurst, T., & Illingworth, G. 2003a, ApJ, 593, 640.

Bouwens, R. J. et al. 2003b, ApJ, 595, 589.

Bouwens, R. J. et al. 2004a, ApJ, 606, L25

Bouwens, R.J., Broadhurst, T.J., Illingworth, G.D., Meurer, G.R., Blakeslee, J.P., Franx, M., & Ford, H.C. 2004b, ApJ, submitted (B04).

Bouwens, R.J., Illingworth, G.D., Blakeslee, J.P., Broadhurst, T.J., & Franx, M. 2004c, ApJ, 611, L1.

Bouwens, R.J. et al. 2004d, in preparation.

Bunker, A.J., Stanway, E.R., Ellis, R.S., McMahon, R.G. 2004, MNRAS, submitted.

Burgasser, A., et al. 2004, in preparation.

Dickinson, M. 2000, Royal Society of London Philosophical Transactions Series A, 358, 2001.

Dickinson, M. et al. 2004, ApJ, 600, L99.

Egami, E. et al. 2004, in preparation.

Ferguson, H. C. et al. 2004, ApJ, 600, L107.

Fernández-Soto, A., Lanzetta, K. M., & Chen, H.-W. 2003, MNRAS, 342, 1215.

Giallongo, E., Cristiani, S., D'Odorico, S., & Fontana, A. 2002, ApJ, 568, L9.

Giavalisco, M. et al. 2004, ApJ, 600, L103.

Knapp, G.R., et al. 2004, AJ, in press.

Kneib, J., Ellis, R. S., Santos, M. R., & Richard, J. 2004, ApJ, 607, 697.

Kogut, A. et al. 2003, ApJS, 148, 161.

Kron, R. G. 1980, ApJS, 43, 305.

Lilly, S.J., Le Fevre, O., Hammer, F., & Crampton, D. 1996, ApJ, 460, L1.

Madau, P., Pozzetti, L. & Dickinson, M. 1998, ApJ, 498, 106.

Pelló, R., Schaerer, D., Richard, J., Le Borgne, J.-F., & Kneib, J.-P. 2004, A&A, 416, L35.

Robberto, M. et al. 2004, in preparation.

Schaerer, D. 2003, A&A, 397, 527.

Somerville, R. S., Lee, K., Ferguson, H. C., Gardner, J. P., Moustakas, L. A., & Giavalisco, M. 2004, ApJ, 600, L171.

Stanway, E. R., Bunker, A. J., & McMahon, R. G. 2003, MNRAS, 342, 439.

Stanway, E. R., Bunker, A. J., McMahon, R. G., Ellis, R. S., Treu, T., & McCarthy, P. J. 2004a, ApJ, 607, 704.

Stanway, E. R., McMahon, R. G., & Bunker, A. J. 2004b, MNRAS, submitted.

Steidel, C. C., Adelberger, K. L., Giavalisco, M., Dickinson, M. and Pettini, M. 1999, ApJ, 519, 1.

Steidel, C. C., Pettini, M., & Adelberger, K. L. 2001, ApJ, 546, 665.

Stiavelli, M., Fall, S. M., & Panagia, N. 2004, ApJ, 610, L1.

Szalay, A.S., Connolly, A.J., & Szokoly, G.P. 1999, AJ, 117, 68.

Thompson, R.I. et al. 2004a, in preparation.

Thompson, R.I. et al. 2004b, in preparation.

Venkatesan, A., Tumlinson, J., & Shull, J. M. 2003, ApJ, 584, 621.

Yan, H., Windhorst, R. A., & Cohen, S. H. 2003, ApJ, 585, L93.

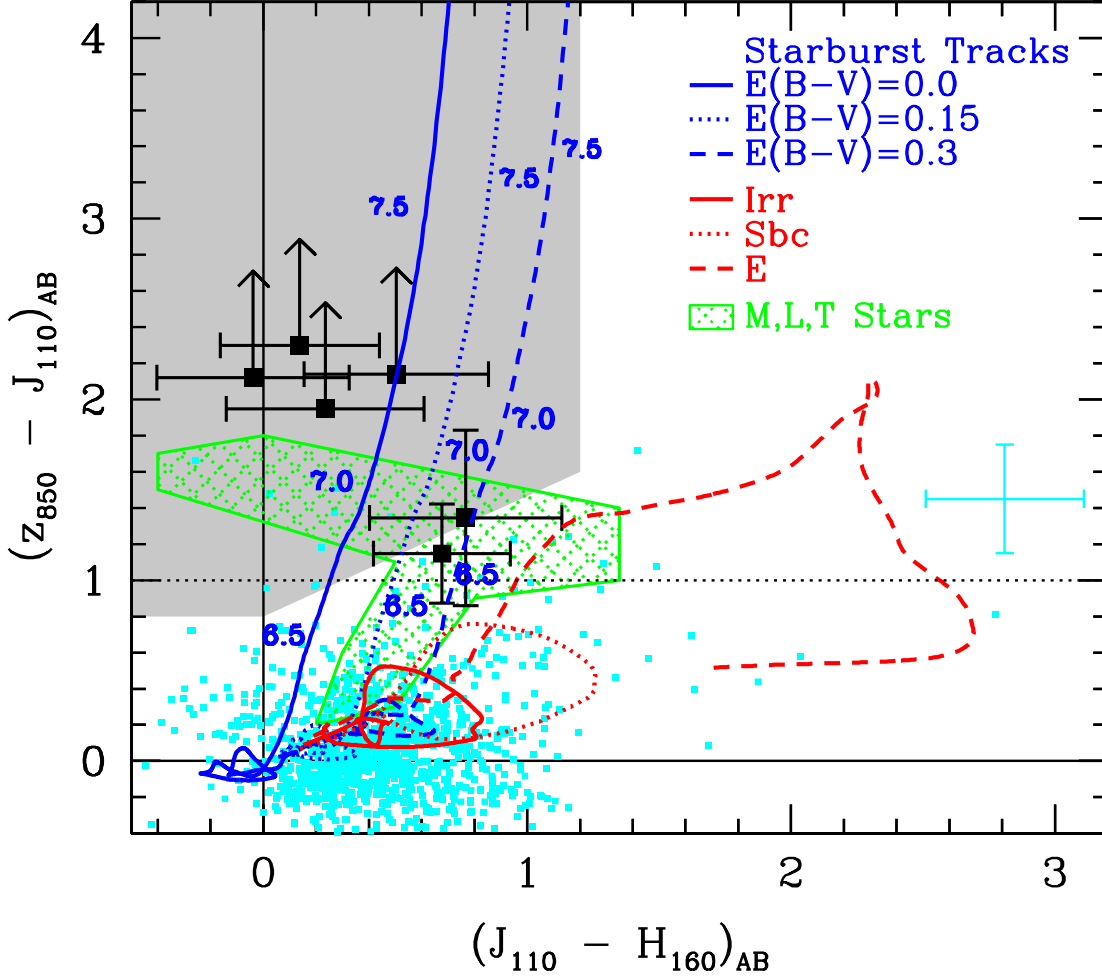Yan, H. & Windhorst, R. A. 2004, ApJ, 612, L93.

Fig. 1.— $(z_{850} - J_{110})_{AB}/(J_{110} - H_{160})_{AB}$ color-color diagram showing the position of our z_{850}-dropouts (selection region is shaded gray) relative to the UDF photometric sample (cyan squares). Objects included in the source list (Table 1) are shown as black squares (2σ lower limits are indicated by vertical arrows). These objects are not detected in the optical V_{606} and i_{606} bands. The cyan squares that lie in the selection region have clear V_{606} and i_{775} detections ($> 2\sigma$) and so are not candidate z_{850}-dropouts; representative error bars for these objects are shown at the right of this diagram. The color-color tracks of both lower redshift interlopers (*red lines*) and 10^8 yr starburst SEDs with different reddenings (*blue lines*) are plotted as a function of redshift. The position of M, L, and T dwarfs are also shown (*green cross hatched region*) (Knapp et al. 2004). Error bars on the $z_{850} - J_{110}$ and $J_{110} - H_{160}$ colors are 1σ.
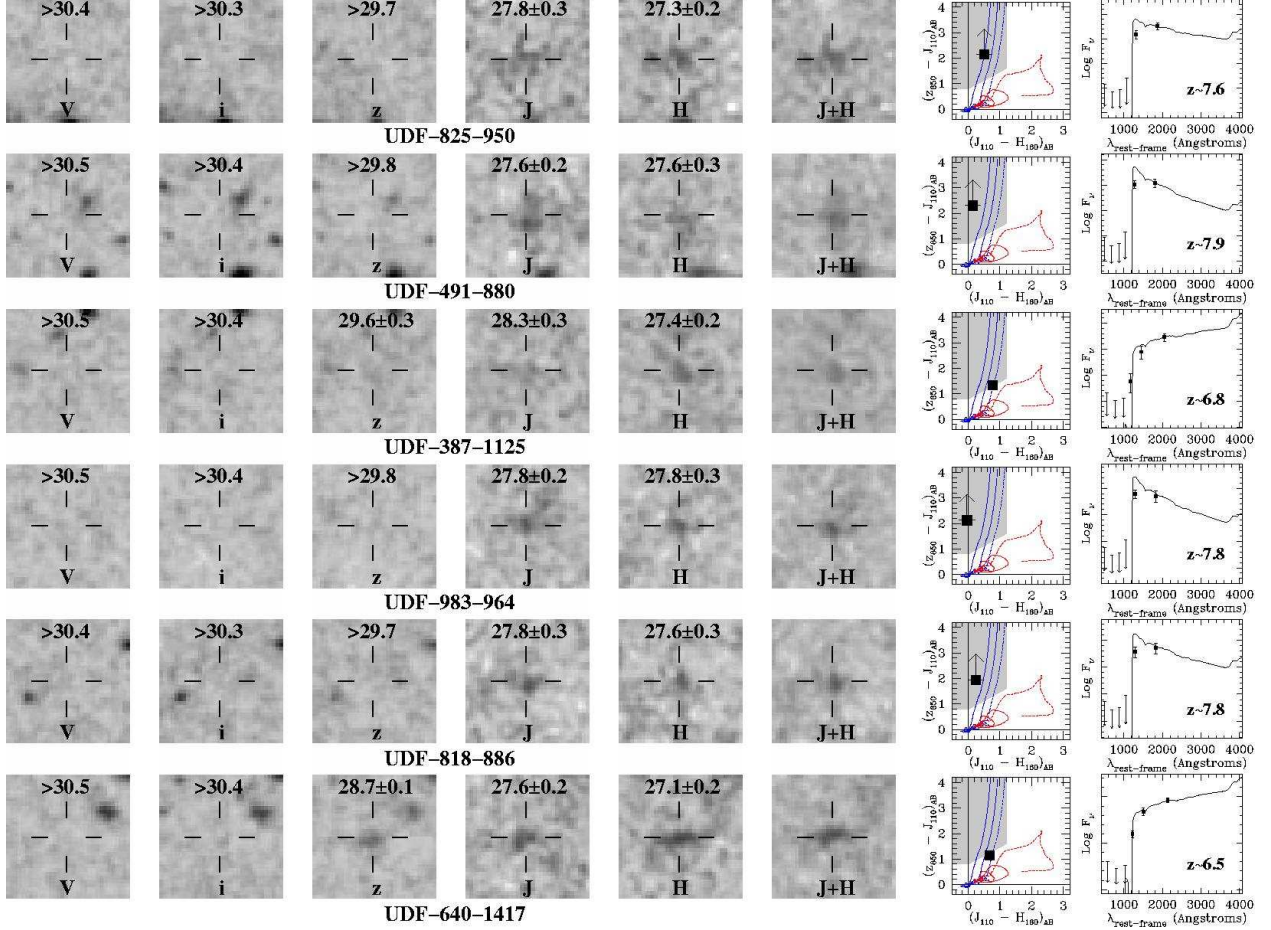
Fig. 2.— Postage stamps images ($V_{606}i_{775}z_{850}J_{110}H_{160}$ bands) of our 5 z_{850}-dropout candidates. Also shown (UDF-640-1417: bottom row) is one very red $(z_{850} - J_{110})_{AB} = 1.1$ object which nearly met our selection criteria and could be a reddened starburst at $z \sim 6.5$ (or a reddened early type at $z \sim 1.6$) (also found by Yan & Windhorst 2004). While our best-fit to UDF-387-1125 is a $z \sim 6.8$ starburst spectrum, this object is also consistent with being a compact $z \sim 1$, $0.01L^*$ dust-reddened early type galaxy. Magnitudes are those measured in a $0.6''$-diameter aperture. The three rightmost panels show the combined $J_{110} + H_{160}$ image for each object, its position in color-color space, and an SED fit to the broadband fluxes. The derived redshift is also provided in the rightmost panel. The ACS cutouts here are shown at a much higher contrast than the NICMOS cutouts, demonstrating the significance of the optical non-detections. The postage stamps are $2.9'' \times 2.9''$ in size. A linear stretch is used for scaling the pixel fluxes.
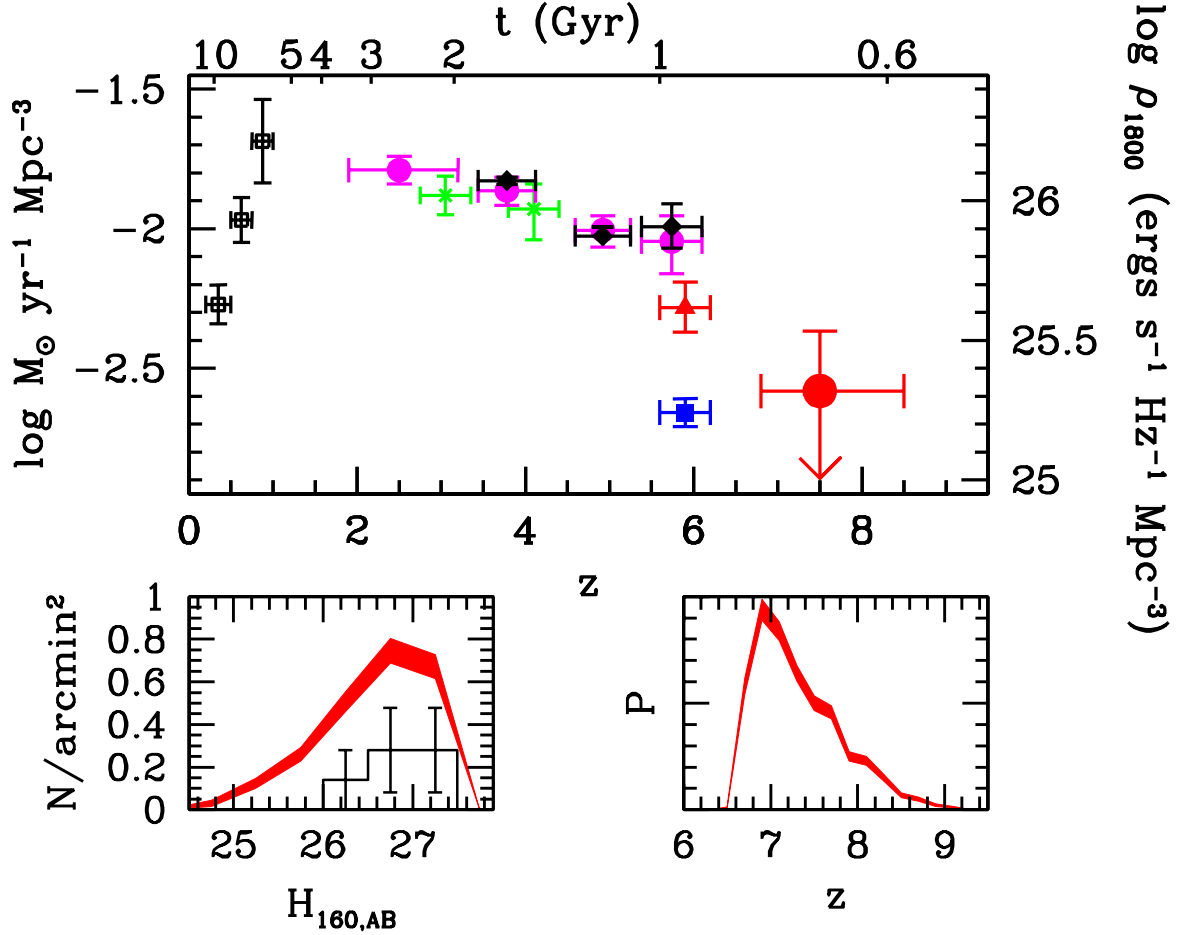
Fig. 3.— Top Panel: Rest-frame continuum UV ($\sim 1800\mathring{A}$) luminosity density (integrated down to 0.3 $L^*_{z=3}$) vs. redshift. The observed luminosity density is converted to a star formation rate (uncorrected for extinction) assuming a Salpeter IMF (e.g., Madau et al. 1998). The present determination (assuming 4 candidates) is shown as the large red circle, with an upper limit shown to acknowledge possible concerns regarding several of our candidates. Previous determinations from Lilly et al. (1996) (*open squares*), Steidel et al. (1999) (*green crosses*), Giavalisco et al. (2004a) (*solid black diamonds*), Bunker et al. (2004) (*solid blue square*), B04 (*solid magenta circles*), and Bouwens et al. 2004a (*solid red triangle*) are also shown. The uncertainty expected from large scale structure (cosmic variance) is ±20% for many of the lower redshift points (e.g., Somerville et al. 2004) and ±50% for the $z \sim 7.5$ point. The top horizontal axis provides the corresponding age of the universe. Lower Left Panel: The surface density vs. total magnitude of the observed z_{850}-dropouts (*histogram*) and that predicted from a $(1+z)^{-1}$ size scaling of our GOODS B-dropout sample (B04) (*red, see §2e*). Lower Right Panel: The expected redshift distribution for z_{850}-dropouts derived from these same simulations. These results suggest a modest to significant decline in the star formation rate density (uncorrected for extinction: see Thompson et al. 2004b for the extinction-corrected star formation history).

Table 1. $z \sim 7 - 8.5$ Sample.[a]

Object ID	Right Ascension	Declination	$H_{160,Cor}$	$H_{160,Ap1}$	$H_{160,Ap2}$	$z - J$	$J - H$	S/G	$r_{hl}('')$
UDF-825-950	03:32:39.538	-27:47:17.41	26.1 ± 0.3	27.3 ± 0.2	26.7 ± 0.2	>2.1	0.5±0.3	0.08	0.39
UDF-491-880[†]	03:32:40.941	-27:47:41.83	26.6 ± 0.3	27.6 ± 0.3	26.9 ± 0.2	>2.3	0.1±0.3	0.03	0.34
UDF-387-1125	03:32:42.565	-27:47:31.42	26.6 ± 0.3	27.4 ± 0.2	27.0 ± 0.2	1.4±0.4	0.8±0.3	0.68	0.28
UDF-983-964	03:32:38.794	-27:47:07.14	27.1 ± 0.3	27.8 ± 0.3	27.1 ± 0.2	>2.1	0.0±0.3	0.48	0.27
UDF-818-886[†]	03:32:39.292	-27:47:22.12	27.1 ± 0.3	27.6 ± 0.3	27.3 ± 0.3	>2.0	0.2±0.3	0.84	0.23
UDF-640-1417[*]	03:32:42.562	-27:46:56.58	26.0 ± 0.3	27.1 ± 0.2	26.5 ± 0.2	1.1±0.2	0.7±0.2	0.11	0.37

[a]All magnitudes are AB magnitudes. Right ascension and declination use the J2000 equinox. Errors are 1σ. Limits on $z_{850} - J_{110}$ colors are 2σ. "S/G" denotes the SExtractor stellarity parameter, for which 0 indicates an extended object, and 1 a point source. "Cor" refers to a total magnitude estimated using the Kron system (see §2), "Ap1" refers to a $0.6''$-diameter aperture magnitude, and "Ap2" refers to a $1.0''$-diameter aperture magnitude. $z - J$ and $J - H$ colors were estimated in a Kron aperture with Kron factor equal to 1.2 (similar to the $0.6''$-diameter apertures used for "Ap1").

[†]These candidates are not found (UDF-818-886) or seen to lower significance (UDF-491-880) in an independent reduction of the NICMOS field kindly provided to us by Robberto et al. (2004).

[*]This object was very close to meeting our selection criteria and could be a reddened starburst at $z \sim 6.5$. Another possibility is that of a dusty/evolved galaxy at $z \sim 1.6$. This object was also found by Yan & Windhorst (2004).